CBGL: Fast Monte Carlo Passive Global Localisation for 2D LIDAR Sensors

Alexandros Filotheou

Abstract—Lorem ipsum dolor sit amet, consectetuer adipiscing elit. Ut purus elit, vestibulum ut, placerat ac, adipiscing vitae, felis. Curabitur dictum gravida mauris. Nam arcu libero, nonummy eget, consectetuer id, vulputate a, magna. Donec vehicula augue eu neque. Pellentesque habitant morbi tristique senectus et netus et malesuada fames ac turpis egestas. Mauris ut leo. Cras viverra metus rhoncus sem. Nulla et lectus vestibulum urna fringilla ultrices. Phasellus eu tellus sit amet tortor gravida placerat. Integer sapien est, iaculis in, pretium quis, viverra ac, nunc. Praesent eget sem vel leo ultrices bibendum. Aenean faucibus. Morbi dolor nulla, malesuada eu, pulvinar at, mollis ac, nulla. Curabitur auctor semper nulla. Donec varius orci eget risus. Duis nibh mi, congue eu, accumsan eleifend, sagittis quis, diam. Duis eget orci sit amet orci dignissim rutrum.

CBGL leverages the relationships of (a) proportionality between the pose estimate error and the value of the Cumulative Absolute Error per Ray (CAER) metric for pose estimates in a neighbourhood of the origin, and (b) lack of disproportionality outside of that neighbourhood

Index Terms—global localisation, 2D LIDAR, monte carlo, scan–to–map-scan matching

I. INTRODUCTION

This paper addresses the problem of Passive Global Localisation of a 2D LIDAR sensor, i.e. the estimation of its location and orientation within a given map, under complete locational and orientational uncertainty, without prescribing motion commands (to the mobile robot that the sensor is assumed mounted to) for further knowledge acquisition. Specifically the problem is formalised in Problem P:

Problem P. Let the unknown pose of an immobile 2D range sensor whose angular range is λ be $\boldsymbol{p}(\boldsymbol{l}, \theta)$, $\boldsymbol{l} = (x, y)$, with respect to the reference frame of map $\boldsymbol{M}$. Let the range sensor measure range scan $\mathcal{S}_R$. The objective is the estimation of $\boldsymbol{p}$ given $\boldsymbol{M}$, λ, and $\mathcal{S}_R$.

II. DEFINITIONS

Let $\mathcal{A} = \{\alpha_i : \alpha_i \in \mathbb{R}\}$, $i \in \mathtt{I} = \langle 0, 1, \ldots, n-1 \rangle$, denote a set of n elements, $\langle \cdot \rangle$ denote an ordered set, $\mathcal{A}_\uparrow$ the set $\mathcal{A}$ ordered in ascending order, the bracket notation $\mathcal{A}[\mathtt{I}] = \mathcal{A}$ denote indexing, and notation $\mathcal{A}_{k:l}$, $0 \le k \le l$, denote limited indexing: $\mathcal{A}_{k:l} = \{\mathcal{A}[k], \mathcal{A}[k+1], \ldots, \mathcal{A}[l]\}$.

Definition I. *Range scan captured from a 2D LIDAR sensor.*—A conventional 2D LIDAR sensor provides a finite number of ranges, i.e. distances to objects within its range, on a horizontal cross-section of its environment, at regular angular and temporal intervals, over a defined angular range [1]. A range scan $\mathcal{S}$, consisting of N_s rays over an angular range λ, is an ordered map $\mathcal{S} : \Theta \to \mathbb{R}_{\ge 0}$, $\Theta = \{\theta_n \in [-\frac{\lambda}{2}, +\frac{\lambda}{2}) : \theta_n = -\frac{\lambda}{2} + \lambda \frac{n}{N_s}, n = 0, 1, \ldots, N_s - 1\}$. Angles
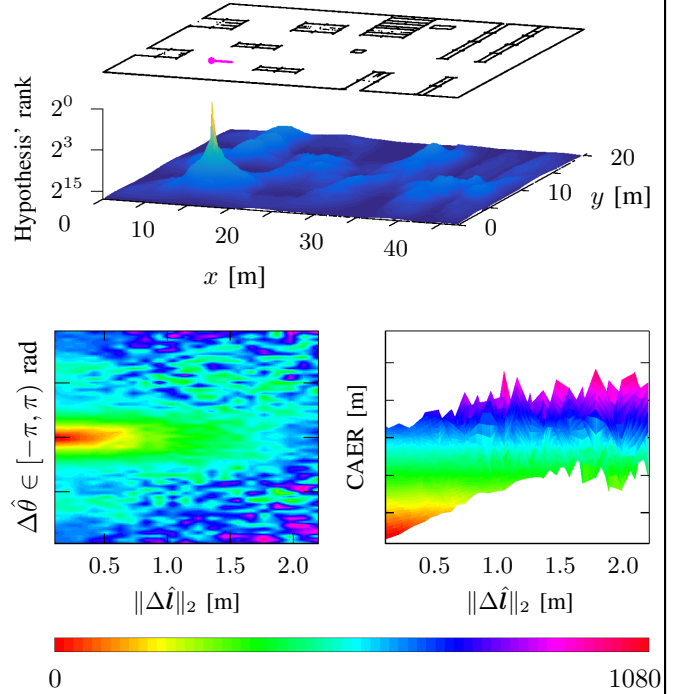

Fig. 1: Given a 2D LIDAR sensor's measurement, at its core, CBGL disperses pose hypotheses within the map and ranks them ascendingly according to the value of the CAER metric, producing a $\mathtt{r}$(ank)-field which may be used to estimate the pose of the sensor quickly due to the low complexity of the CAER metric. Top: a map of an environment, the pose of a panoramic 2D LIDAR sensor (magenta), and the corresponding CAER rank field below them. Bottom: distribution of CAER values by location and orientation error of all sensor pose hypotheses corresponding to the rank field above, for estimate distances up to 2.0 m. In this example the map's area is 800 m², and 10^6 hypotheses were dispersed randomly in its free space for 100 times; CBGL's maximum location error and maximum execution time were, respectively, 0.062 m and 8.8 sec

θ_n are expressed relative to the sensor's heading, in the sensor's frame of reference.

Definition II. *Map-scan.*—A map-scan is a virtual scan that encapsulates the same pieces of information as a scan derived from a physical sensor. Only their underlying operating principle is different due to the fact the map-scan refers to distances to the boundaries of a point-set, referred to as the map, rather than within a real environment. A map-scan $\mathcal{S}_V^M(\hat{\boldsymbol{p}})$ is derived by means of locating intersections of rays emanating from the estimate of the sensor's pose estimate $\hat{\boldsymbol{p}}$ and the boundaries of the map $\boldsymbol{M}$.

Definition III. *CAER as metric.*—Let $\mathcal{S}_p$ and $\mathcal{S}_q$ be two range scans, equal in angular range λ and size N_s. The value

of the Cumulative Absolute Error per Ray (CAER) metric $\psi \in \mathbb{R}_{\geq 0}$ between $\mathcal{S}_p$ and $\mathcal{S}_q$ is given by

$$\psi(\mathcal{S}_p, \mathcal{S}_q) \triangleq \sum_{n=0}^{N_s-1} \left| \mathcal{S}_p[n] - \mathcal{S}_q[n] \right| \qquad (1)$$

Definition IV. *CAER as field.*—A ψ-field on map $\boldsymbol{M}$ $f_\psi^{\boldsymbol{M}} : \mathbb{R}^2 \times [-\pi, +\pi) \to \mathbb{R}_{\geq 0}$ is a mappping of 3D pose configurations $\hat{\boldsymbol{p}}(\hat{x}, \hat{y}, \hat{\theta})$ to CAER values (def. III) such that if $\psi(\mathcal{S}_R, \mathcal{S}_V^{\boldsymbol{M}}(\hat{\boldsymbol{p}})) = c$ then $f_\psi^{\boldsymbol{M}}(\hat{\boldsymbol{p}}) = c$. In other words a CAER field is produced by computing the value of the CAER metric between a range scan $\mathcal{S}_R$ (def. I) and a map-scan $\mathcal{S}_V^{\boldsymbol{M}}(\hat{\boldsymbol{p}})$ captured from pose configuration $\hat{\boldsymbol{p}}$ within map $\boldsymbol{M}$ (def. II).

Definition V. *Rank field.*—Let $f_\psi^{\boldsymbol{M}}$ be a ψ-field on map $\boldsymbol{M}$ and $\mathcal{P} = \{\hat{\boldsymbol{p}}_i\}$, $i \in \mathtt{I} = \langle 0, 1, \ldots, |\mathcal{P}| - 1 \rangle$, be a set of 3D pose configurations within map $\boldsymbol{M}$, such that $f_\psi^{\boldsymbol{M}}(\mathcal{P}) = \Psi$. Let $\mathtt{I}^*$ be the set of indices such that $\Psi[\mathtt{I}^*] = \Psi_\uparrow$. A r-field on map $\boldsymbol{M}$ $f_r^{\boldsymbol{M}} : \mathbb{R}^2 \times [-\pi, +\pi) \to \mathbb{Z}_{\geq 0}$ is a mapping of 3D pose configurations $\mathcal{P}$ to non-negative integers such that if $f_\psi^{\boldsymbol{M}}(\mathcal{P}) = f_\psi^{\boldsymbol{M}}(\mathcal{P}[\mathtt{I}]) = \Psi$ then $f_r^{\boldsymbol{M}}(\mathcal{P}[\mathtt{I}^*]) = \mathtt{I}$. In other words a rank field maps the elements of pose estimate set $\{\hat{\boldsymbol{p}}_i\}$ to the ranks $\mathtt{I}^*$ of their corresponding CAER values in hierarchy $\Psi_\uparrow$.

Definition VI. *Field densities.*—The locational and angular density, d_l and d_α respectively, of a ψ- or r-field express, correspondingly, the number of pose estimates per unit area of space and 2π rad.

III. Related Work
IV. The CBGL method

The proposed method's foundations rest on observation O:

Observation O. It may be observed that there are conditions such that hypothesis H stands true.

Hypothesis H. There exists $\overline{\delta} \in \mathbb{R}_{>0}$ such that conjecture

Conjecture C. Let the unknown pose of a 2D range sensor measuring range scan $\mathcal{S}_R$ (def. I) be $\boldsymbol{p}(x, y, \theta)$ with respect to the reference frame of map $\boldsymbol{M}$. Let $\mathcal{H}$ be a set of pose hypotheses within the free (i.e. traversable) space of $\boldsymbol{M}$: $\mathcal{H} = \{\hat{\boldsymbol{p}}_i(\hat{x}_i, \hat{y}_i, \hat{\theta}_i)\} \subseteq \mathtt{free}(\boldsymbol{M})$, $i \in \mathtt{I} = \langle 0, 1, \ldots, |\mathcal{H}| - 1 \rangle$. Let $f_\psi^{\boldsymbol{M}}$ be the ψ-field on $\boldsymbol{M}$ (def. IV) and $f_r^{\boldsymbol{M}}$ be the corresponding r-field (def. V) such that $f_\psi^{\boldsymbol{M}}(\mathcal{H}) = \Psi$, $\Psi[\mathtt{I}^*] = \Psi_\uparrow$, and $f_r^{\boldsymbol{M}}(\mathcal{H}[\mathtt{I}^*]) = \mathtt{I}$. Let $\mathcal{V} = \{\hat{\boldsymbol{p}}_i \in \mathcal{H} : \|\boldsymbol{p} - \hat{\boldsymbol{p}}_i\|_2 < \delta_0$ and $\psi(\mathcal{S}_R, \mathcal{S}_V^{\boldsymbol{M}}(\hat{\boldsymbol{p}}_i)) < \psi_0\}$. Without loss of generality there exist $\delta_0, \psi_0 \in \mathbb{R}_{>0}$ such that for all $\hat{\boldsymbol{p}}_\mathcal{V} \in \mathcal{V}$

$$f_\psi^{\boldsymbol{M}}(\hat{\boldsymbol{p}}_\mathcal{V}) < f_\psi^{\boldsymbol{M}}(\hat{\boldsymbol{p}}) \quad \Leftrightarrow$$
$$f_r^{\boldsymbol{M}}(\hat{\boldsymbol{p}}_\mathcal{V}) < f_r^{\boldsymbol{M}}(\hat{\boldsymbol{p}}) \quad \Leftrightarrow$$
$$\|\boldsymbol{p} - \hat{\boldsymbol{p}}_\mathcal{V}\|_2 < \|\boldsymbol{p} - \hat{\boldsymbol{p}}\|_2$$

for any $\hat{\boldsymbol{p}} \in \mathcal{H} \setminus \mathcal{V} : \|\boldsymbol{p} - \hat{\boldsymbol{p}}\|_2 \geq \delta_0$.

Remark I. The composition of $\mathcal{H} = \mathcal{V} \cup \mathcal{X} \cup \mathcal{W}$, where $\mathcal{X} = \hat{\boldsymbol{p}} \in \mathcal{H} \setminus \mathcal{V} : \|\boldsymbol{p} - \hat{\boldsymbol{p}}\|_2 \geq \delta_0$ and $\mathcal{W} = \hat{\boldsymbol{p}} \in \mathcal{H} \setminus \mathcal{V} : \|\boldsymbol{p} - \hat{\boldsymbol{p}}\|_2 < \delta_0$. With respect to set $\mathcal{W}$ ... ??

Algorithm I: CBGL

Input: $\mathcal{S}_R$, $\boldsymbol{M}$, $|\mathcal{H}|$, ∇
Output: $\hat{\boldsymbol{p}}$

1: $\mathcal{H} \leftarrow \{\varnothing\}$
2: **for** $i \leftarrow 0, 1, \ldots, |\mathcal{H}| - 1$ **do**
3: $\quad \hat{\boldsymbol{p}}_i \leftarrow \mathtt{rand}(\hat{x}, \hat{y}, \hat{\theta}) : (x, y) \in \mathtt{free}(\boldsymbol{M})$
4: $\quad \mathcal{H} \leftarrow \{\mathcal{H}, \hat{\boldsymbol{p}}_i\}$
5: **end for**
6: $\mathcal{H}_1 \leftarrow \mathtt{bottom\_n\_poses}(\mathcal{S}_R, \boldsymbol{M}, \mathcal{H}, \nabla)$ $\quad$ (Alg. II)
7: $\mathcal{H}_2 \leftarrow \{\varnothing\}$
8: **for** $k \leftarrow 0, 1, \ldots, |\mathcal{H}_1| - 1$ **do**
9: $\quad \hat{\boldsymbol{h}}' \leftarrow \mathtt{sm2}(\mathcal{S}_R, \boldsymbol{M}, \mathcal{H}_1[k])$ $\quad$ (Alg. III or e.g. x1 [2])
10: $\quad \mathcal{H}_2 \leftarrow \{\mathcal{H}_2, \hat{\boldsymbol{h}}'\}$
11: **end for**
12: $\hat{\boldsymbol{p}} \leftarrow \mathtt{bottom\_n\_poses}(\mathcal{S}_R, \boldsymbol{M}, \mathcal{H}_2, 1)$
13: **return** $\hat{\boldsymbol{p}}$

Algorithm II: bottom_n_poses

Input: $\mathcal{S}_R$, $\boldsymbol{M}$, $\mathcal{H}$, ∇
Output: $\mathcal{H}_\nabla$

1: $\Psi \leftarrow \{\varnothing\}$
2: **for** $h \leftarrow 0, 1, \ldots, |\mathcal{H}| - 1$ **do**
3: $\quad \mathcal{S}_V^h \leftarrow \mathtt{scan\_map}(\boldsymbol{M}, \mathcal{H}[h])$
4: $\quad \psi \leftarrow 0$
5: $\quad$ **for** $n \leftarrow 0, 1, \ldots, |\mathcal{S}_R| - 1$ **do**
6: $\quad\quad \psi \leftarrow \psi + \left| \mathcal{S}_R[n] - \mathcal{S}_V^h[n] \right|$ $\quad$ (Eq. (1))
7: $\quad$ **end for**
8: $\quad \Psi \leftarrow \{\Psi, \psi\}$
9: **end for**
10: $[\Psi_\uparrow, \mathtt{I}^*] \leftarrow \mathtt{sort}(\Psi, \mathtt{asc})$
11: $\mathcal{H}_\nabla \leftarrow \{\varnothing\}$
12: **for** $h \leftarrow 0, 1, \ldots, \nabla - 1$ **do**
13: $\quad \mathcal{H}_\nabla \leftarrow \{\mathcal{H}_\nabla, \mathcal{H}[\mathtt{I}^*[h]]\}$
14: **end for**
15: **return** $\mathcal{H}_\nabla$

Algorithm III: sm2

Input: $\mathcal{S}_R$, $\boldsymbol{M}$, $\hat{\boldsymbol{p}}$
Output: $\hat{\boldsymbol{p}}'$

1: $\mathcal{S}_V \leftarrow \mathtt{scan\_map}(\boldsymbol{M}, \hat{\boldsymbol{p}})$
2: $\boldsymbol{\Delta p} \leftarrow \mathtt{scan\text{-}match}(\mathcal{S}_R, \mathcal{S}_V)$ $\quad$ (e.g. ICP [3], FSM [4])
3: $\hat{\boldsymbol{p}}' \leftarrow \hat{\boldsymbol{p}} + \boldsymbol{\Delta p}$
4: **return** $\hat{\boldsymbol{p}}'$
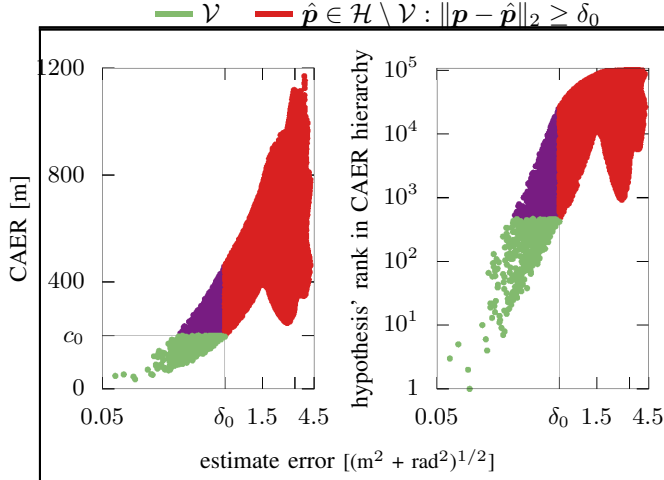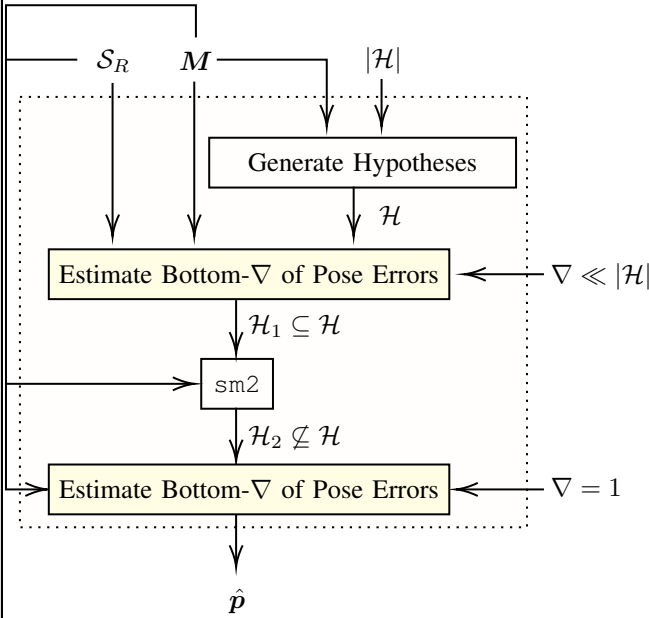
Fig. 2:

Fig. 4:

Fig. 3:

V. Experimental Evaluation

VI. Characterisation & Limitations

VII. Conclusion

References

[1] M. Cooper, J. Raquet, and R. Patton, "Range Information Characterization of the Hokuyo UST-20LX LIDAR Sensor," *Photonics*, 2018.

[2] A. Filotheou, A. L. Symeonidis, G. D. Sergiadis, and A. G. Dimitriou, "Correspondenceless scan-to-map-scan matching of 2d panoramic range scans," *Array*, vol. 18, 2023.

[3] I. Vizzo, T. Guadagnino, B. Mersch, L. Wiesmann, J. Behley, and C. Stachniss, "Kiss-icp: In defense of point-to-point icp simple, accurate, and robust registration if done the right way," *IEEE Robotics and Automation Letters*, 2023.

[4] A. Filotheou, G. D. Sergiadis, and A. G. Dimitriou, "Fsm: Correspondenceless scan-matching of panoramic 2d range scans," in *2022 IEEE/RSJ International Conference on Intelligent Robots and Systems (IROS)*, 2022.
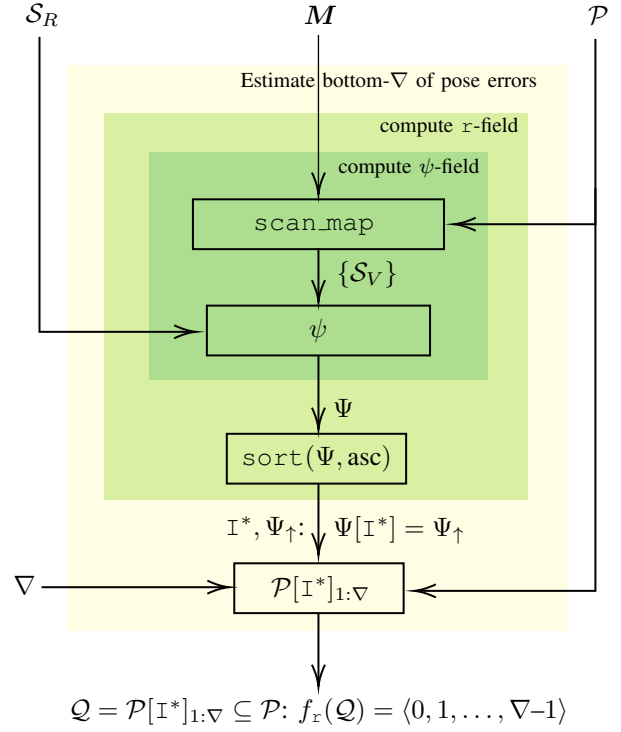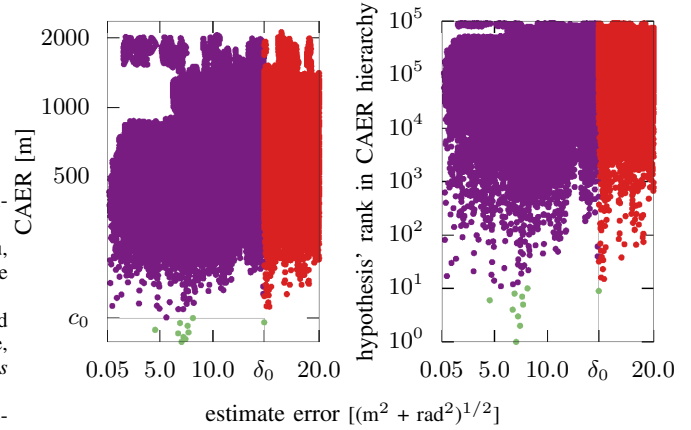
Fig. 5: